Stanford Exploration Project, Report 117, October 23, 2004, pages 141–150

Stanford Exploration Project, Report 117, October 23, 2004, pages 141–150

Midpoint-offset vs. source-receiver coordinates for PEF-based interpolation

William Curry[1]

ABSTRACT

There are two obvious choices of coordinates to use when interpolating seismic data: cmp-offset and source-receiver. A multi-scale prediction-error filter (PEF) based interpolation works well on both sets of coordinates for a 2D prestack land dataset, although the cmp-offset coordinates appear to be preferable. By using reciprocity in source-receiver space, a pair of 2D PEFs may interpolate the data with more efficiency and practical applicability to 3D data.

INTRODUCTION

Interpolation of reflection seismic data is performed in many different ways, including kinematically (Chemingui, 1999; Fomel, 2001; Biondi and Vlad, 2001), with high-resolution radon-based methods (Sacchi and Ulrych, 1995; Trad et al., 2002; Trad, 2003), with Fourier-domain methods (Schonewille, 2000; Zwartjes and Hindriks, 2001; Liu, 2004), and with prediction-error filter (PEF) based methods (Spitz, 1991; Claerbout, 1999; Crawley, 2000).

PEF-based methods can now deal with irregularly-sampled data (Curry and Brown, 2001; Curry, 2002), where multiple rescaled copies of the data are used to estimate a non-stationary PEF. This multi-scale methodology has been shown to work on sparse synthetic data.

I use the multi-scale method on a prestack 2D land dataset from Colombia. The data suffers from many missing shots but the receiver coverage is relatively uniform, meaning that in source-receiver coordinates only one axis is poorly-sampled. In cmp-offset coordinates the coverage is not uniform in either the cmp or the offset axes. The multi-scale PEF estimation should be robust to this problem, however.

I test the interpolation with non-stationary, multi-scale PEFs in both source-receiver as well as cmp-absolute offset coordinates. In source-receiver coordinates, additional traces predicted by reciprocity are added, so that the known data looks like a grid of crossing tracks. The crossing tracks are quite reminiscent of the Madagascar interpolation problem (Ecker and Berlioux, 1995; Lomask, 1998, 2002; Curry, 2004; Lomask, 2004). I also propose a method using two orthogonal 2D non-stationary single-scale PEFs, based largely on a proposed method for the Madagascar problem (Curry, 2004).

[1]**email:** bill@sep.stanford.edu

BACKGROUND

Prediction-error filter (PEF) based interpolation can be cast as a two stage linear least-squares process (Claerbout, 1999), where a PEF is first estimated on the known data. Then, the output of convolution of the newly-found PEF with the desired model is minimized while fixing the known data. The first stage of the process can be described mathematically by

$$\mathbf{W}(\mathbf{DKf}+\mathbf{d}) \approx \mathbf{0}, \tag{1}$$

where the known data ($\mathbf{d}$) is convolved ($\mathbf{D}$) with a PEF with unknown coefficients ($\mathbf{f}$), except for the first, which is constrained by $\mathbf{K}$ to be 1. If there are areas where the filter is being convolved with unknown data, those areas are weighted to 0 by a diagonal weight $\mathbf{W}$. The second stage can be described by

$$\begin{aligned} \mathbf{L_{data}m} &= \mathbf{d} \\ \mathbf{Fm} &\approx \mathbf{0}. \end{aligned} \tag{2}$$

In the second fitting goal, $\mathbf{L}$ is a selector matrix that is 1 where there is a data point and 0 where there isn't, $\mathbf{m}$ is the interpolated output, $\mathbf{d}$ is once again the known data, and $\mathbf{F}$ represents convolution with the newly-found PEF.

In the case of a non-stationary PEF, where the filter varies with position, a second fitting goal has to be added to the first stage of the interpolation process, so that the now much greater number of filter coefficients becomes adequately constrained. This fitting goal can be expressed as

$$\mathbf{Af} \approx \mathbf{0}, \tag{3}$$

where $\mathbf{A}$ is a regularization operator (typically a Laplacian) that operates spatially over each filter coefficient separately, and $\mathbf{f}$ is the non-stationary PEF. Fitting goal (1) is written identically for the non-stationary case, but each of the operators present (as well as the filter) are now non-stationary. A full description of what the matrices for non-stationary PEFs look like is given in SEP-113 (Guitton, 2003).

Typically, when interpolating data that are regularly-sampled, the filter is interlaced so that the filter skips over the missing traces, which allows a filter to be estimated (Crawley, 2000). Once the filter has been estimated, the interlacing of the filter is undone for the second stage of the interpolation process.

When the data are not regularly-sampled, the interlacing approach usually fails. In this case, a multi-scale approach can be used where a non-stationary PEF can be estimated on multiple regridded copies of the original data (Curry and Brown, 2001; Curry, 2002, 2003). This can be expressed as

$$\mathbf{W}\left(\begin{bmatrix} \mathbf{D_0} \\ \mathbf{D_1} \\ \mathbf{D_2} \\ \cdots \\ \mathbf{D_n} \end{bmatrix} \mathbf{KPf} + \begin{bmatrix} \mathbf{d_0} \\ \mathbf{d_1} \\ \mathbf{d_2} \\ \cdots \\ \mathbf{d_n} \end{bmatrix}\right) \approx \mathbf{0}. \tag{4}$$

Here, the different scales of data $\mathbf{D_i}$ are generated by the normalized adjoint of linear interpolation, which takes points from a fine grid and sprays them into the coarser grid, then normalizes by the fold. The weight $\mathbf{W}$ is now a diagonal weight for all scales of data, while the introduction of a sub-sampling operator $\mathbf{P}$ subsamples the non-stationary filter so that the spatial size of the filter will match the size of the rescaled data.

Another possible approach is to use a pair of non-stationary 2D PEFs which are estimated independently from the original unscaled data using fitting goals (1) and (3) in two different directions. Once these two PEFs have been estimated, they could be used in tandem to interpolate missing data by (Claerbout, 1999; Curry, 2004):

$$\begin{aligned} \mathbf{L_{data}m} &\approx \mathbf{d} \\ \epsilon_x \mathbf{F_x m} &\approx \mathbf{0} \\ \epsilon_y \mathbf{F_y m} &\approx \mathbf{0}, \end{aligned} \tag{5}$$

where $\mathbf{F_x}$ and $\mathbf{F_y}$ are 2D non-stationary PEFs (compared to the typically-3D PEF shown before in fitting goal 2), $\mathbf{L_{data}}$ selects known data points, $\mathbf{d}$ is still the known data and $\mathbf{m}$ the unknown model. Unlike the multi-scale approach, this method requires that the data are evenly-sampled along tracks oriented in two different directions.

EXAMPLE

The data set used in this paper is a 2D land dataset from Colombia. There are approximately 300 shots with a nominal spacing of 50 m, 350 receivers in a split-spread with a spacing of 25 m, and a time sampling of 4 ms. A fold diagram of the acquisition is shown in Figure 1. As seen in the figure, there is almost no irregularity in the receiver positions, excluding the lack of very near offsets. However, the source positions in the survey are quite irregular, as shown by the gaps in the vertical axis.

When examining the spatial distribution of the data in cmp and offset coordinates (Figure 2), the irregularity of the source positions can be seen in both the cmp and offset positions. In Figure 2, the data are shown in cmp and absolute offset coordinates, as the sign of the offset of a trace is unimportant if reciprocity is assumed. The receiver cables that appear as horizontal lines in Figure 1 now appear as diagonal lines in cmp-absolute offset space. However, since this is split-spread land data, the negative offsets appear as diagonal lines running orthogonal to the positive offsets, with the 'reflecting point' of this line occurring at zero absolute offset.

The orthogonal tracks caused by the split-spread acquisition are very reminiscent of the crossing tracks shown in the Madagascar satellite dataset (Ecker and Berlioux, 1995). It is possible that methods being developed for this data would also be applicable to split-spread land data. When looking at the spatial distribution of this land data in source-receiver coordinates and by adding a second set of traces predicted by reciprocity, two sets of crossing horizontal and vertical lines can be observed, shown in Figure 3.

A window was selected from both the cmp-absolute offset and the source-receiver cube, that was $200 \times 100 \times 100$ both for both display and computational concerns. The two cubes

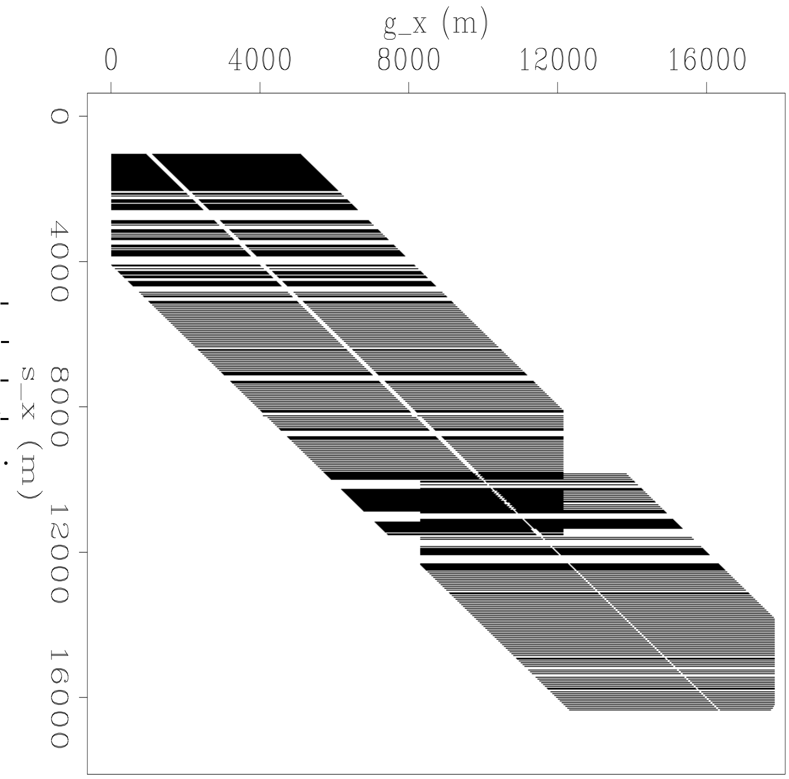

Figure 1: A map of source and receiver positions. Receivers are well-sampled, as shown in the horizontal axis. The source sampling is irregular, as seen in the vertical axis.. bill1-sg-fold [ER]

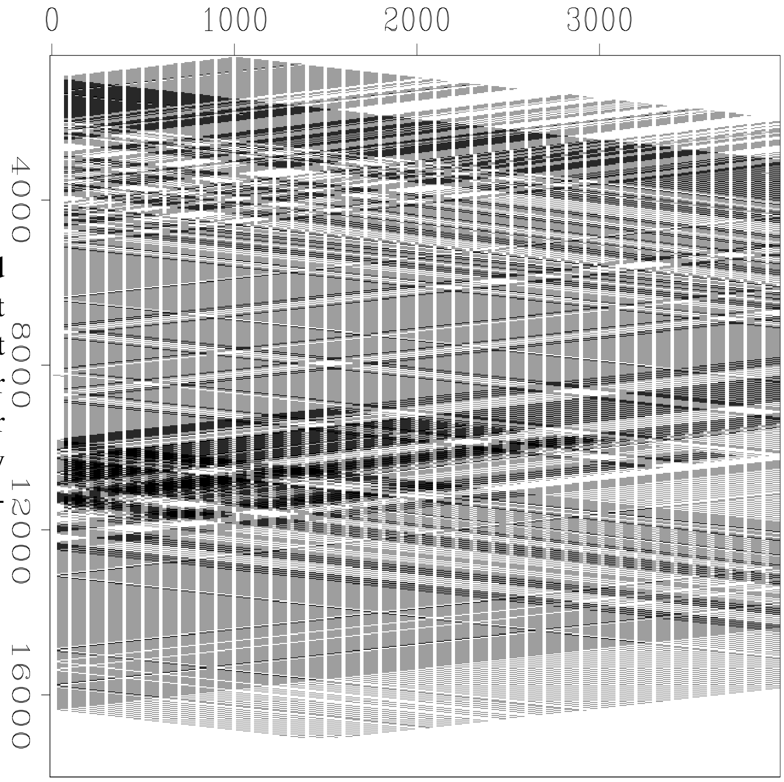

Figure 2: A map of midpoint and absolute offset positions. The split spread is shown by the two different orientations of a receiver line, one for the positive offsets and another for the negative offsets. The irregularity in sources leads to gaps in both directions. bill1-co-fold [ER]

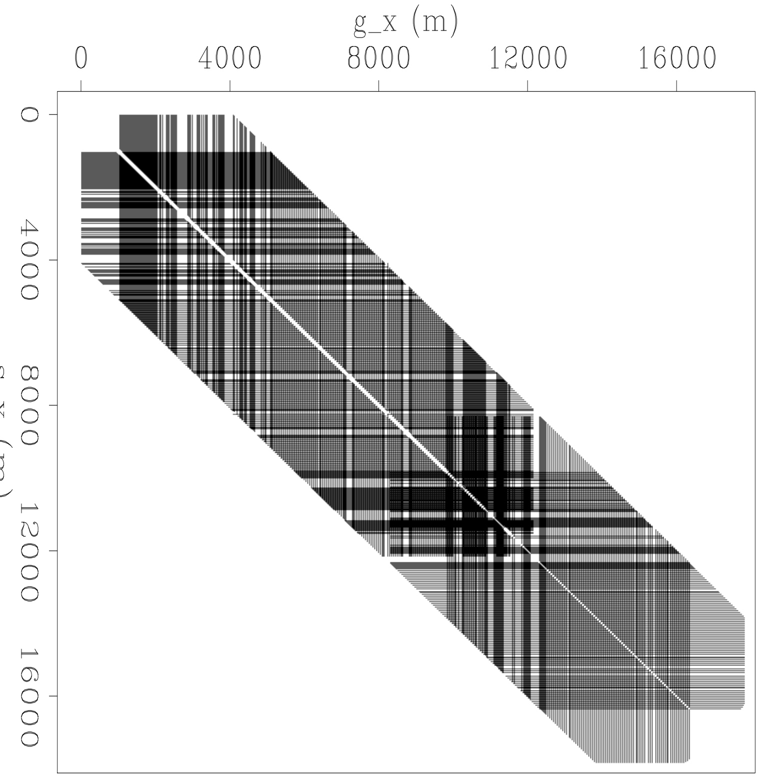

Figure 3: A map of source and receiver positions, including a second set of traces predicted by reciprocity. This second set intersects with the first set because both positive and negative offsets are present. bill1-sg-rec-fold [ER]

are somewhat co-located, and contain small as well as large gaps. In both domains a 3D non-stationary $10 \times 3 \times 3$ coefficient PEF was estimated with 5 scales of data. The filter had micropatches (Crawley, 2000) of size $5 \times 5 \times 5$, Laplacian regularization with an identical ϵ, and 100 iterations of a conjugate-gradient solver were used to estimate the PEFs.

For the second stage of the interpolation (after the PEF has been estimated), fitting goals (2) were solved in each domains with 100 iterations of a conjugate-gradient solver.

The results from the cmp-absolute offset domain interpolation are shown in Figure 4. The interpolation is quite successful. While in the common offset section there does not appear to be that many discernible features to interpolate, the cmp gather has multiple simultaneous dips (some steep) that are interpolated correctly, as well as a range of gap sizes.

The results of the interpolation in source-receiver coordinates are shown in Figure 5. In this domain, absent sources appear as empty boxes within the data cube, whereas the same holes are roughly diamond-shaped in cmp-absolute offset space. The interpolated results are acceptable, but are not as impressive as those in cmp-absolute offset space. This could be because of the distribution of the data, and the fact that the square-shaped holes would lead to coarser scales of data dominating the estimation in source-receiver coordinates compared to cmp-absolute offset coordinates.

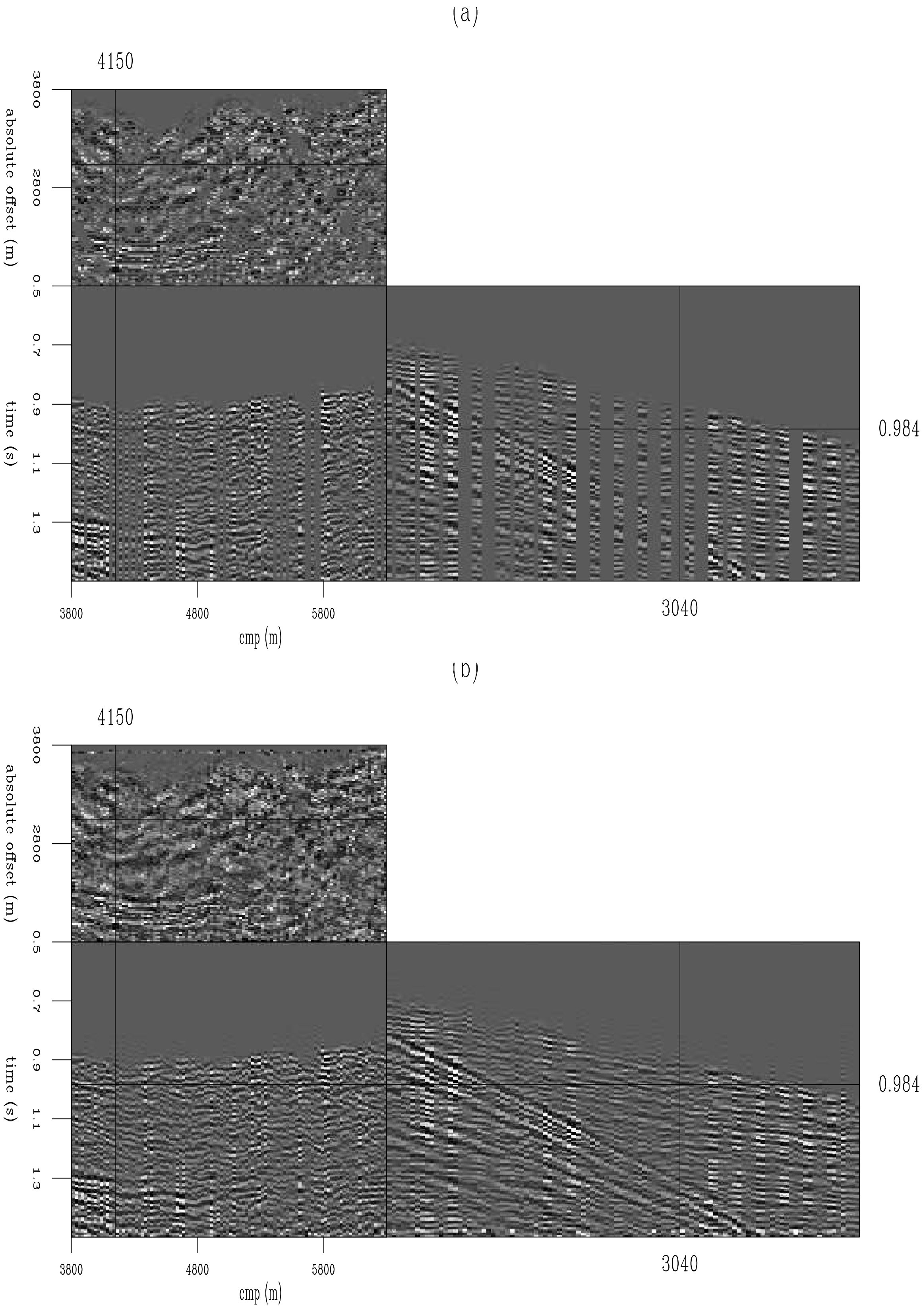

Figure 4: Interpolation in cmp-absolute offset coordinates, (a): Original data, (b): Interpolated data. bill1-cmp-interp [CR,M]

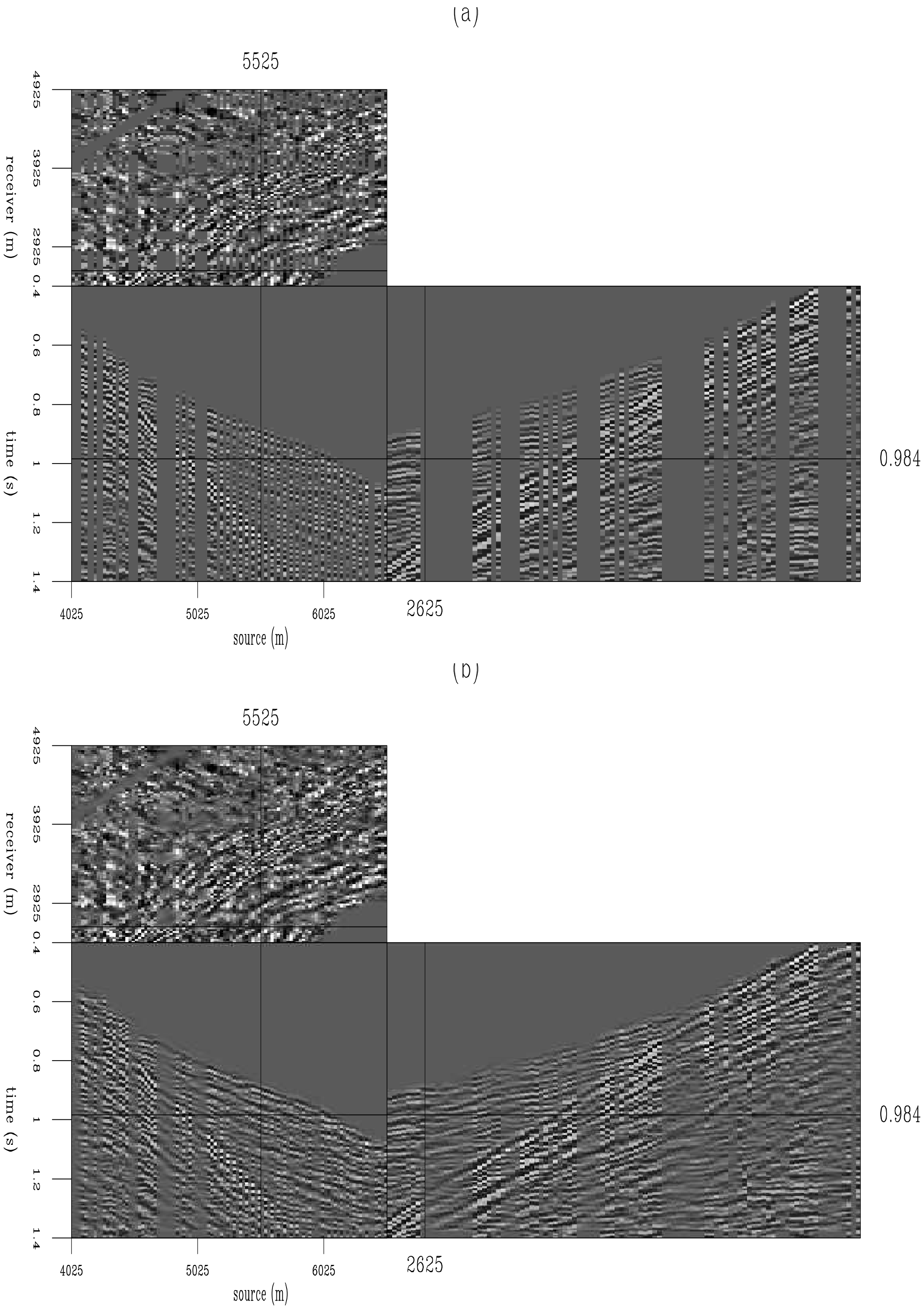

Figure 5: Interpolation in source-receiver coordinates, (a): Original data, (b): Interpolated data. bill1-sg-interp [CR,M]

CONCLUSIONS AND FUTURE WORK

Multi-scale PEF-based interpolation in both the cmp-absolute offset and source-receiver coordinates appear to yield acceptable results, although the cmp-absolute offset result is noticeably better. Using CMP-absolute offset coordinates has the benefit of being a smaller space to operate in. However, by using source-receiver coordinates, an interpolation scheme with two 2-D PEFs could be used, which would almost exactly match the distribution of the data compared to the random-sampling assumption made with the multi-scale approach. This would be substantially less expensive as no rescaling would be necessary.

The two most pressing future directions for this work are the applicability of these methods to 3D prestack data, and the effect of the different interpolations on the final migrated image.

ACKNOWLEDGMENTS

I would like to thank Ecopetrol for providing the data used in this paper.

REFERENCES

Biondi, B., and Vlad, I., 2001, Amplitude preserving prestack imaging of irregularly sampled 3-D data: SEP–**110**, 1–18.

Chemingui, N., 1999, Imaging irregularly sampled 3D prestacked data: Ph.D. thesis, Stanford University.

Claerbout, J., 1999, Geophysical estimation by example: Environmental soundings image enhancement: Stanford Exploration Project, `http://sepwww.stanford.edu/sep/prof/`.

Crawley, S., 2000, Seismic trace interpolation with nonstationary prediction-error filters: Ph.D. thesis, Stanford University.

Curry, W., and Brown, M., 2001, A new multiscale prediction-error filter for sparse data interpolation: SEP–**110**, 113–122.

Curry, W., 2002, Non-stationary, multi-scale prediction-error filters and irregularly sampled data: SEP–**111**, 327–337.

Curry, W., 2003, More fitting equations for PEF estimation on sparse data: SEP–**114**, 171–176.

Curry, W., 2004, Regularizing madagascar: Pefs from the data space?: SEP–**115**, 347–356.

Ecker, C., and Berlioux, A., 1995, Flying over the ocean southeast of Madagascar: SEP–**84**, 295–306.

Fomel, S., 2001, Three-dimensional seismic data regularization: Ph.D. thesis, Stanford University.

Guitton, A., 2003, Multiple attenuation with multidimensional prediction-error filters: SEP–**113**, 57–74.

Liu, B., 2004, Multi-dimensional reconstruction of seismic data: Ph.D. thesis, University of Alberta.

Lomask, J., 1998, Madagascar revisited: A missing data problem: SEP–**97**, 207–216.

Lomask, J., 2002, Madagascar satellite data: An inversion test case: SEP–**111**, 337–349.

Lomask, J., 2004, Estimating a 2D stationary PEF on sparse data: SEP–**117**.

Sacchi, M. D., and Ulrych, T. J., 1995, High-resolution velocity gathers and offset space reconstruction: Geophysics, **60**, no. 04, 1169–1177.

Schonewille, M., 2000, Fourier reconstruction of irregularly sampled seismic data: Ph.d. thesis: Delft University of Technology.

Spitz, S., 1991, Seismic trace interpolation in the F-X domain: Geophysics, **56**, no. 06, 785–794.

Trad, D., Ulrych, T. J., and Sacchi, M. D., 2002, Accurate interpolation with high-resolution time-variant Radon transforms: Geophysics, **67**, no. 2, 644–656.

Trad, D. O., 2003, Interpolation and multiple attenuation with migration operators: Geophysics, **68**, no. 6, 2043–2054.

Zwartjes, P., and Hindriks, C., 2001, Regularising 3-D data using Fourier reconstruction and sparse inversion: Soc. of Expl. Geophys., 71st Ann. Internat. Mtg, 1906–1909.